

# Dispersions of alkyl-capped silicon nanocrystals in dilute organic solvent/water mixtures: steady-state photoluminescence and ageing studies

Fiona M. Dickinson, Thomas A. Alsop, Naif Al-Sharif, Christine E. M. Berger, Harish K. Datta, Lidija Šiller, Yimin Chao, Eimer M. Tuite, Andrew Houlton and Benjamin R. Horrocks<sup>1</sup>

## Supporting Information

### Contents

<b>1</b>	<b>Methods</b>	<b>2</b>
1.1	Photoemission spectroscopy . . . . .	2
1.2	Raman and Luminescence Spectroscopy . . . . .	2
1.3	Infrared Spectroscopy . . . . .	2
<b>2</b>	<b>Additional Supporting Data</b>	<b>2</b>
2.1	Photoemission spectroscopy . . . . .	2
2.2	Infrared spectroscopy . . . . .	3
2.3	Raman - Luminescence Microscopy . . . . .	4
2.4	X-ray Diffraction (XRD) . . . . .	6
2.5	Scanning transmission electron microscopy (STEM) . . . . .	7
2.6	Atomic force microscopy . . . . .	8
2.7	Uptake of alkyl-SiNCs by HeLa cells - additional data and controls . . . . .	10

This supporting information file provides microscopic and spectroscopic characterisation of the alkyl-capped silicon nanocrystals (alkyl-SiNCs) demonstrating the crystallinity of the Si core and the presence of the alkyl capping monolayer. According to these measurements, the particles have about the same size and structure as those reported in ref. [1].

Finally, additional data showing the uptake of alkyl-SiNCs by HeLa cells from THF/water dispersions is presented. This data also shows the toxicity of THF towards the cells, which is absent in similar images obtained using ether as the vehicle to disperse alkyl-SiNCs in the medium.

---

<sup>1</sup>b.r.horrocks@ncl.ac.uk

# 1 Methods

## 1.1 Photoemission spectroscopy

Photoemission spectra of C<sub>11</sub>-SiNCs were taken using synchrotron radiation at beamline I511 of MAX-Lab, Lund, Sweden. 140 eV photons were used in the Si2p spectra and 354 eV photons were used in the C1s region. The sample was prepared by evaporation of a thick film of SiNCs from a solution in dichloromethane onto a gold nitride foil. Detailed photoemission studies of our SiNCs have been published elsewhere.[1, 2]

## 1.2 Raman and Luminescence Spectroscopy

A CRM200 confocal Raman microscope (Witec GmbH, Ulm, Germany) was used to capture Raman and luminescence spectra. The 488 nm line of an argon ion laser provided the excitation light and the emitted and/or scattered light passed through a Raman edge filter to remove elastically scattered light. The filtered light was collected by a multimode optical fiber which served also as the confocal pinhole. The collected light was analysed by a spectrograph containing a cooled CCD with typical settings for luminescence experiments of: 150 lines/mm (grating) and an integration time of 1 s, or 1800 lines/mm (grating) and 10 s of integration. Gold nitride films were used, rather than pure gold, as substrates for Raman spectroscopy because the morphology of these films produces a significant SERS enhancement: the preparation and characterization of these films has been reported elsewhere.[3]

## 1.3 Infrared Spectroscopy

C<sub>11</sub>-SiNCs were dried on an Si(100) chip and the infrared spectrum was measured in normal transmission mode. The clean Si(100) chip was used to obtain the background. The instrument was a Bio-Rad Excalibur with an MCT detector and 32 scans at 4 cm<sup>-1</sup> resolution were co-added and averaged.

# 2 Additional Supporting Data

The chemical composition of the SiNCs was confirmed by photoemission and infrared spectroscopy to consist of a silicon core covalently bound to saturated C<sub>11</sub> alkyl chains. The crystalline nature of the silicon core was confirmed by Raman spectroscopy, X-ray diffraction (powder patterns) and high resolution scanning transmission electron microscopy. The Scherrer equation was used to extract the diameter of the Si core from the XRD powder pattern linewidths and the value of 2.6 nm was broadly consistent with the electron microscopy and previous estimates from probe microscopy.[2]

## 2.1 Photoemission spectroscopy

Figure 1 shows Si 2p and C 1s spectra of SiNCs deposited as a thick film on a gold nitride foil. As we have discussed previously, such samples are very insulating and the binding energies and peak widths are strongly affected by

changes in screening effects as the film thickness varies. The peak position of ca 103 eV is, in fact, due to unoxidised Si despite the binding energy being higher than for single crystal Si.[2] The presence of oxide, Si(+4), would be signalled by the appearance of a second peak shifted positive of the Si(0) peak by about 3.3 eV. The breadth of the Si 2p peak does however mean that we cannot rule out sub stoichiometric quantities of oxide - this is indeed observed in the FTIR data below.

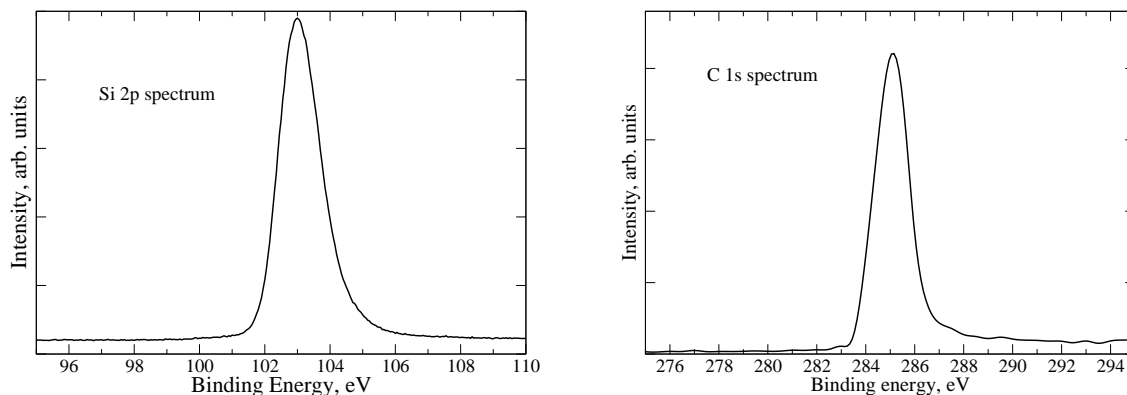


Figure 1: Photoemission spectra of C11- SiNCs on a gold nitride foil. Left: Si 2p spectrum obtained in normal emission using 140 eV photons; Right: C 1s spectrum obtained in normal emission using 354 eV photons

## 2.2 Infrared spectroscopy

Figure 2 shows an infrared spectrum of a dry film of alkyl-SiNCs.

Features characteristic of the saturated alkyl capping layer:

- (1) absence of vinylic C-H stretches at  $3080\text{ cm}^{-1}$  and the sharp C=C stretch at  $1640\text{ cm}^{-1}$  indicates there are no  $\text{sp}^2$  carbon atoms;
- (2) aliphatic C-H stretches in the range  $2960 - 2850\text{ cm}^{-1}$  (including the feature due to methyl groups at  $2960\text{ cm}^{-1}$ ) and the methylene scissor mode at ca.  $1470\text{ cm}^{-1}$  are characteristic of an n-alkyl layer;
- (3) broadened Si-H stretching feature at ca  $2100\text{ cm}^{-1}$  which is characteristic of residual Si-H on alkylated silicon [4] and (4) the broad feature at ca.  $1050\text{ cm}^{-1}$  and the small feature at ca.  $2250\text{ cm}^{-1}$  confirms the presence of a small amount of silicon oxide. The coverage of oxide is much less than that of alkyl chains based on the relative intensities of the features due to  $\text{O}_n\text{Si-H}$  and Si-H stretching modes (which have similar oscillator strengths [5]) as well as the Si-O and C-H features (the Si-O str has a very large oscillator strength).

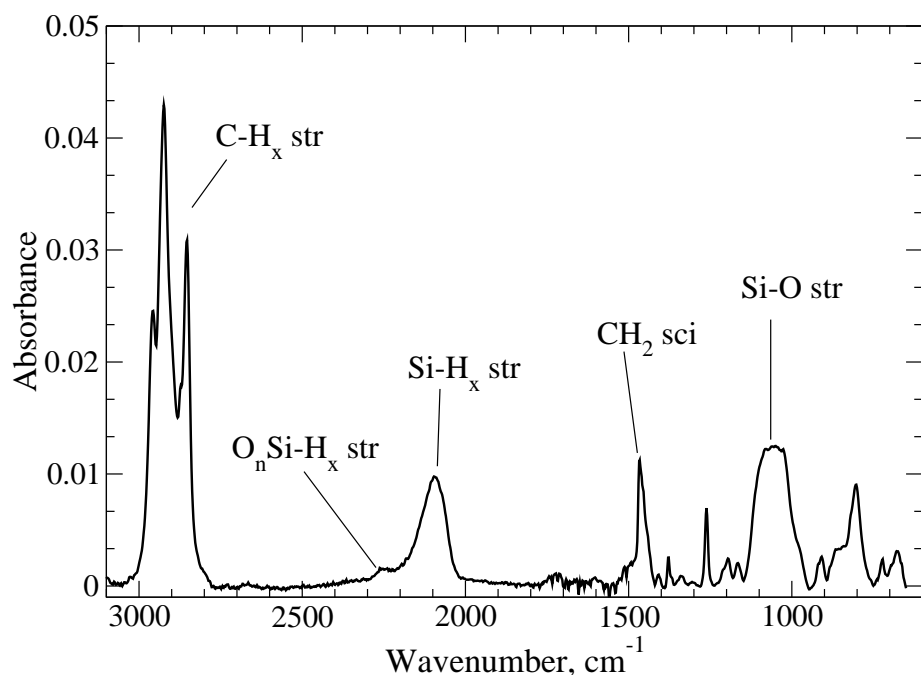


Figure 2: FTIR spectrum in normal transmission of C<sub>11</sub>-SiNCs deposited from dichloromethane solution on a 1 cm<sup>2</sup> Si(100) chip. The background was the same chip before deposition of the alkyl-SiNCs.

### 2.3 Raman - Luminescence Microscopy

Figure 3 shows a luminescence and Raman spectrum of C<sub>11</sub>-SiNCs deposited on a gold nitride foil from dichloromethane solution. An Ar-ion laser (488 nm) line was used to excite the luminescence and two spectra are shown: one was obtained using a 150 line / mm grating which allows collection of both Raman and luminescence from the particles; the other employed a 1800 line / mm grating to show the Raman peak due to the Si at a Raman shift of 515 cm<sup>-1</sup> in greater detail (figure 4). The dark count readings of the CCD have been subtracted from both spectra.

The Raman feature at 515 cm<sup>-1</sup> is characteristic of crystalline silicon and the shift to lower wavenumber than the bulk value is typical of quantum-confined silicon nanocrystals.[6, 7, 8] The luminescence peak position is also consistent with the Si core diameter (ca. 2.5-2.6 nm) determined by XRD linewidth analysis and electron microscopy in the sections below.

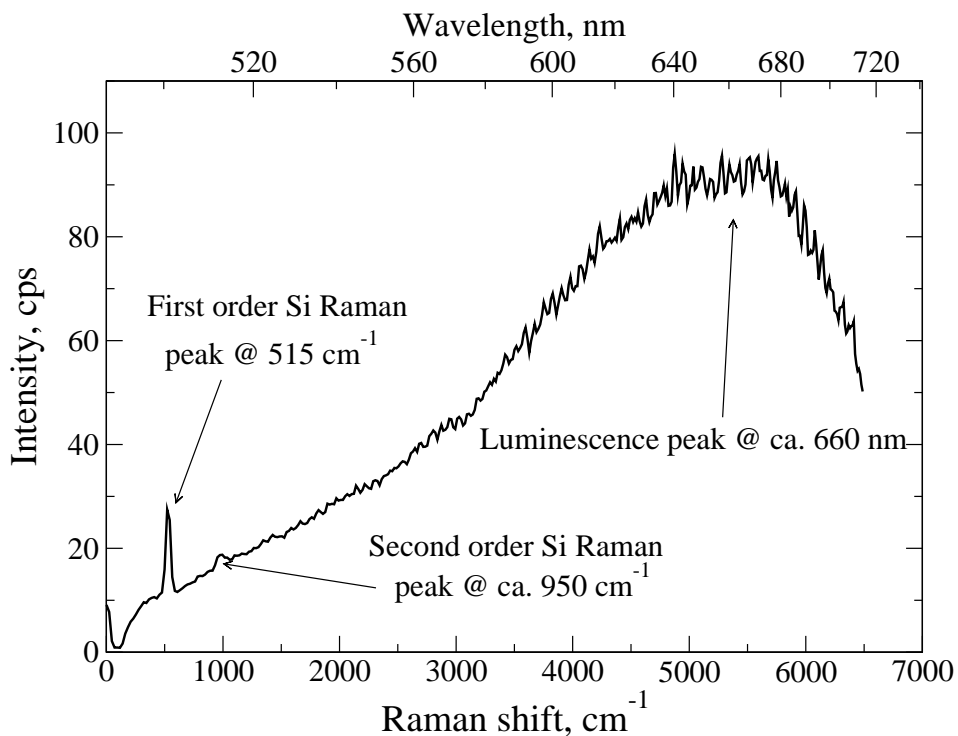


Figure 3: Raman and luminescence spectrum of SiNCs deposited as a film on gold nitride from a solution in dichloromethane. Excitation wavelength = 488 nm, grating = 150 lines / mm.

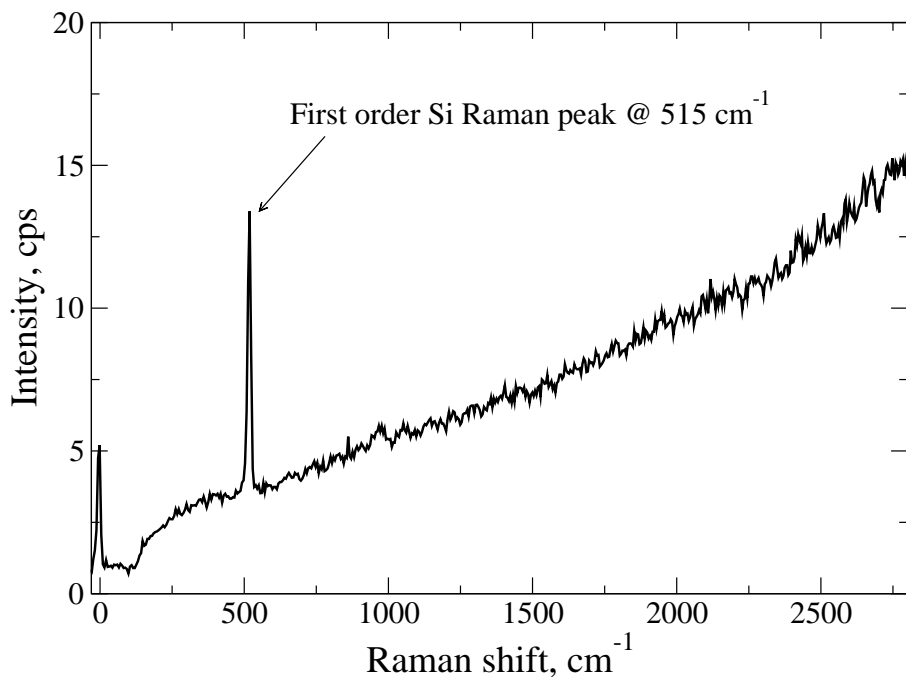


Figure 4: Raman and luminescence spectrum of SiNCs deposited as a film on gold nitride from a solution in dichloromethane. Excitation wavelength = 488 nm, grating = 1800 lines / mm.

## 2.4 X-ray Diffraction (XRD)

XRD pattern for C<sub>11</sub>-SiNCs cast as a film from solution in dichloromethane (figure 5). The peak positions were assigned by comparison with a crystalline Si primary reference: Natl. Bur. Stand. (U.S.) Monogr. 25, 13, 35, (1976).

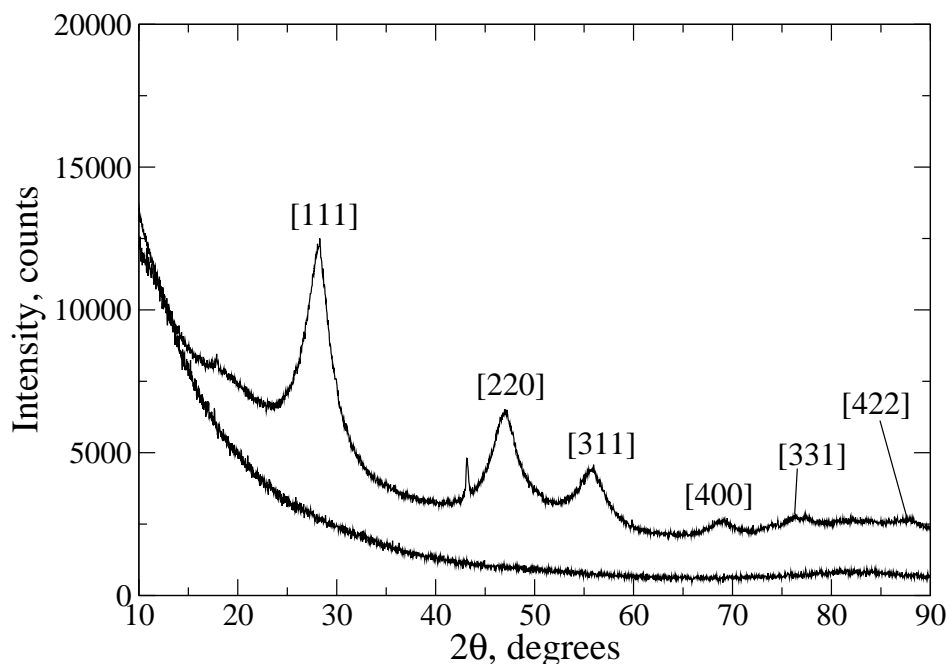


Figure 5: XRD pattern of a film of C<sub>11</sub>-NCs cast from dichloromethane solution. The peaks are assigned to the indicated lattice planes of crystalline silicon. The lower curve is the background scattering from the blank.

Figure 5 shows the expected peaks corresponding to crystalline silicon<sup>2</sup>. The feature at  $2\theta \simeq 28$  degrees due to [111] planes was fitted with a pseudo-Voigt function (figure 6). Using the Scherrer formula and the peak width from the fit, the Si particle diameter (assumed equal to that of the crystallite) is 2.6 nm. The value deduced from the feature at 47 degrees was the same.

---

<sup>2</sup>The small feature at  $2\theta = 43$  degrees is due to a trace of Cu on the sample stage.

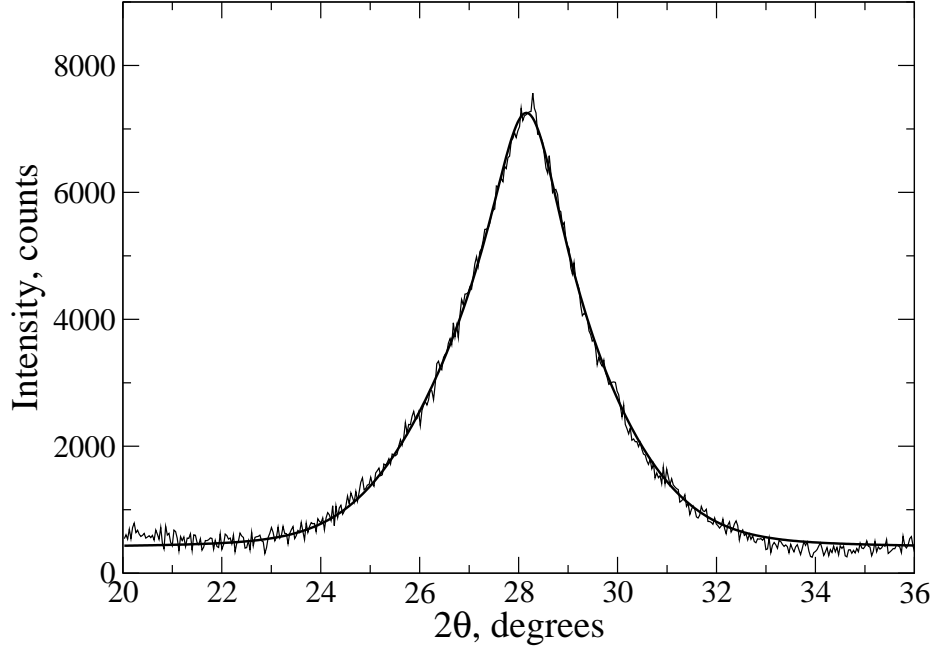


Figure 6: Pseudo-Voigt fit to the (111) peak of the XRD pattern for  $C_{11}$ -NCs after subtraction of a linear baseline.

## 2.5 Scanning transmission electron microscopy (STEM)

Further support for the particle size measurements and the crystallinity of the SiNCs was obtained from scanning transmission electron microscopy. The experiments were carried out in the aberration-corrected Daresbury Super-STEM (Daresbury Laboratory, CCLRC, Daresbury, UK). High resolution bright field and high angle annular dark field (HAADF) images, the latter revealing atomic Z-contrast, were taken simultaneously.

Figure 7 (left) shows a typical high resolution STEM HAADF (aberration-corrected) image of a single  $C_{11}$ -SiNC on a carbon grid. The sample was prepared by placing a drop of dichloromethane solution of  $C_{11}$ -SiNCs on a standard carbon grid. The particle is roughly spherical and the diameter is about 2.5 nm. Electron energy loss spectra (Si L edge) were used to confirm that the white area in the image corresponds to the Si core. A detailed STEM and EEL study will be published elsewhere.

We also obtained high resolution bright-field STEM images of  $C_{11}$ -SiNCs (figure 7, right) that were evaporated at 200°C in UHV and collected on a carbon grid.[1] The presence of Si was confirmed by electron energy loss spectra (Si L edge) and the direct observation of lattice fringes of the appropriate spacing ([100] planes). The image quality is slightly better than for the material deposited from solution; this is probably due to the removal of trace solvent - previously reported to affect the imaging of SiNCs [9] - as the UHV chamber is pumped down.

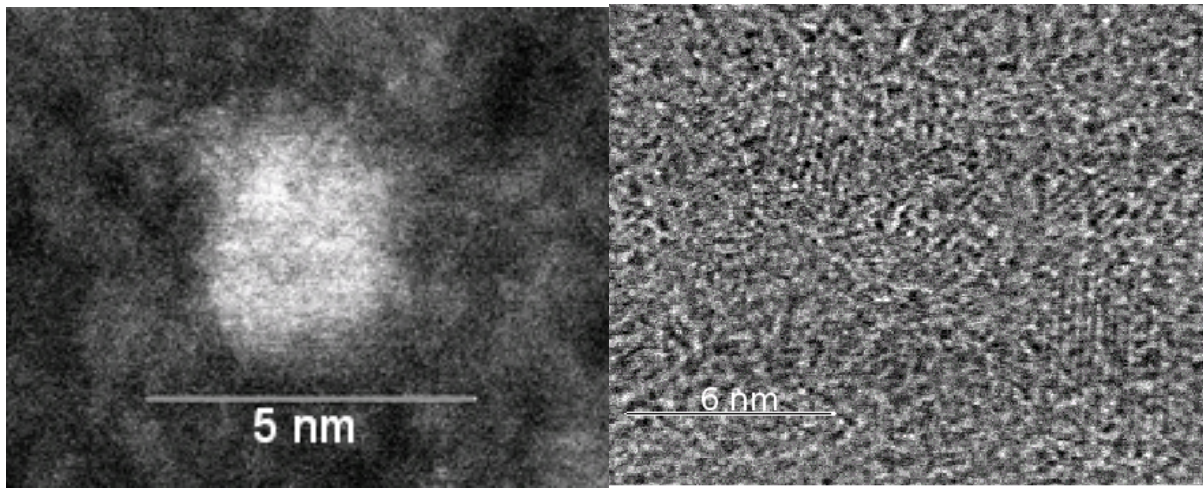


Figure 7: Left: STEM HAADF (aberration-corrected) images of a single  $C_{11}$ -SiNC particle; the white region corresponds to the Si core. Right: bright field image showing several particles in which the lattice fringes due to [001] planes are visible. In both cases, the beam energy was 100 keV and the resolution was about 0.1 nm.

## 2.6 Atomic force microscopy

Figure 8 shows tapping mode AFM images of alkyl-SiNCs deposited on undecyl-capped Si(111) surfaces. These surfaces are very flat, stable and are chemically similar to the undecyl-capped SiNCs. This facilitates height measurements ( $\simeq 5$ nm) of the particles; although the particles do have a tendency to form clusters on the surface, some isolated particles or islands one particle high are detectable (line section (B)).



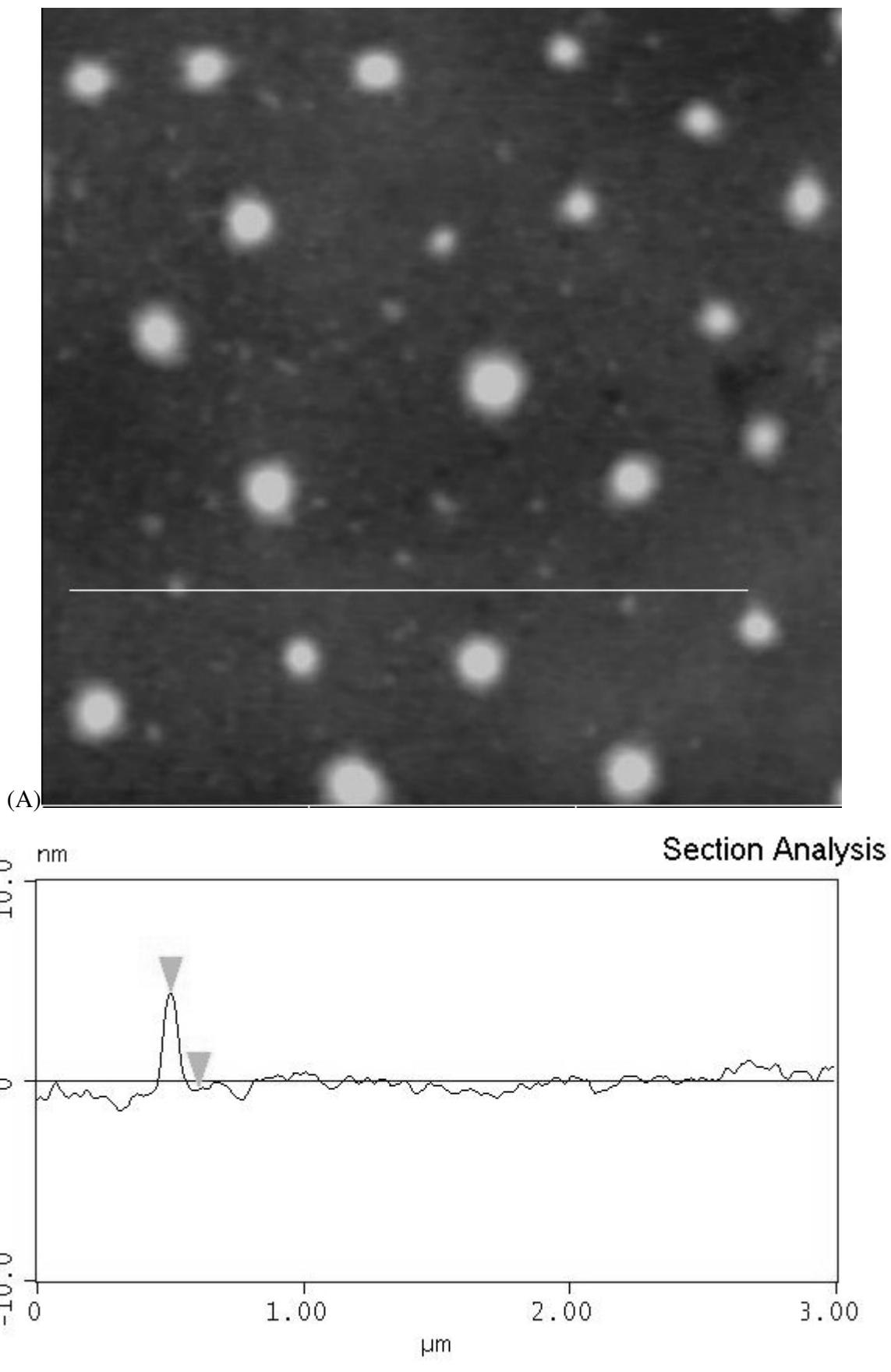


Figure 8: (A) Tapping mode AFM image of alkyl-SiNCs deposited from the vapor onto undecyl-capped Si(111) surfaces. The grayscale corresponds to 20 nm and the image area is  $3 \times 3 \mu\text{m}$ . (B) zoom and line section of an island one particle high.

## 2.7 Uptake of alkyl-SiNCs by HeLa cells - additional data and controls

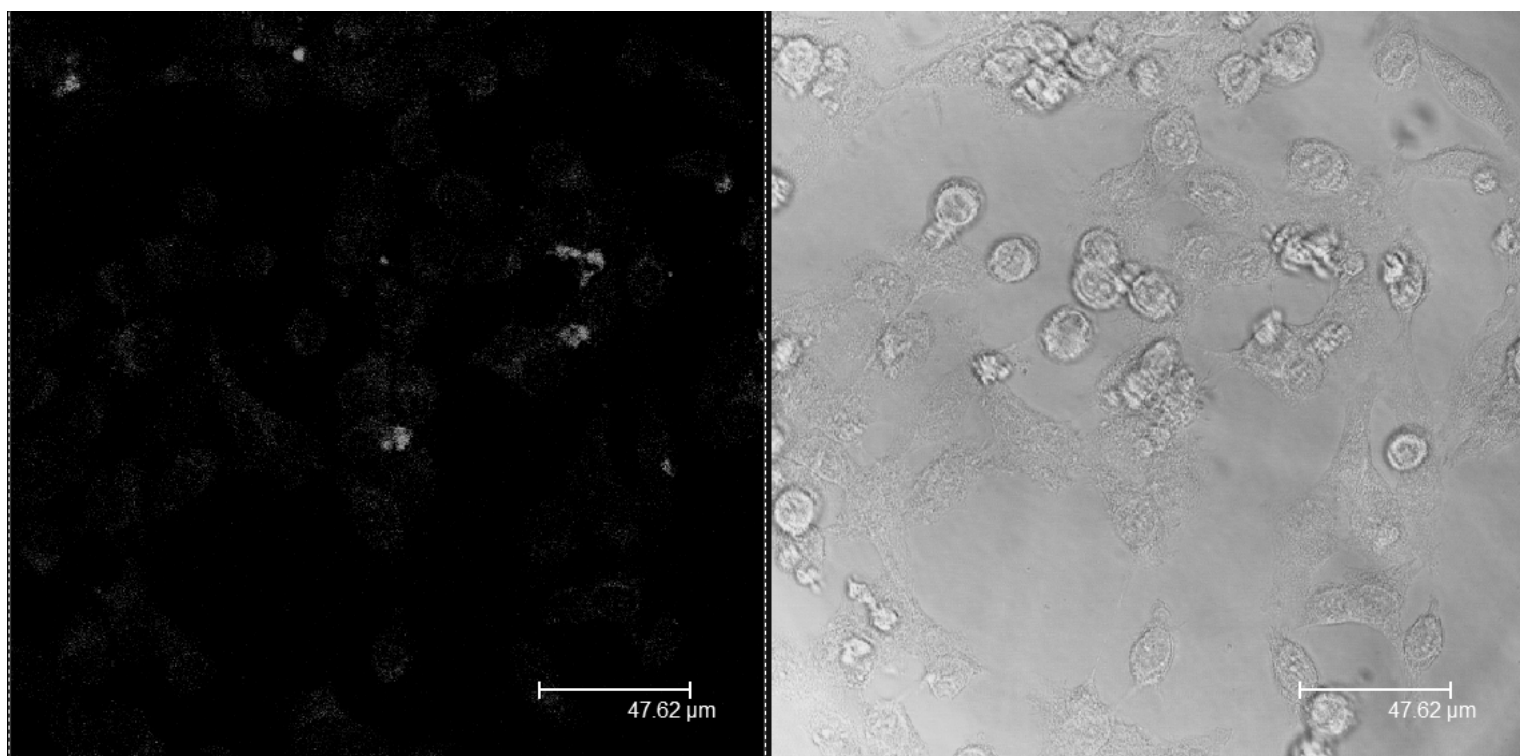


Figure 9: Confocal luminescence images and normal optical images of a field of HeLa cells after incubation in the presence of 0.2% THF v/v for 2h.

Figure 9 shows a confocal fluorescence image ( $\lambda_{ex} = 488$  nm; emission bandpass = 550-650 nm) of HeLa cells after 2h exposure to alkyl-SiNCs ( $\approx 5$  pmol) in 0.2% THF / medium. The cells all show strong luminescence because of internalization of the alkyl-SiNCs, but about 30% of those in the field also show very evident necrosis (rounded appearance). When ether is used as the vehicle, no necrosis or other acute toxicity is observed; a detailed account of this data will be published elsewhere.

Figure 10 shows three images (i) bright-field optical micrograph of HeLa cells; (ii) control confocal fluorescence image of the cells after exposure to the vehicle with no SiNCs and (iii) the confocal fluorescence image of the cells after 2h exposure to SiNCs. The three images do not show the same field, but are all taken from the same sample of HeLa cells before and after treatments with vehicle and vehicle+SiNCs. The emission from the SiNCs is sufficiently bright and far removed (in energy terms) from any autofluorescence to make the contribution of autofluorescence to the images negligible.

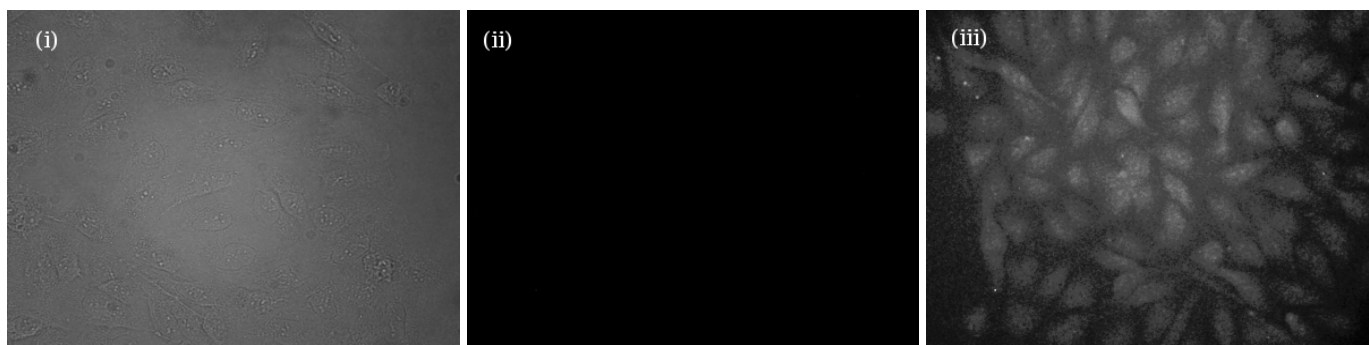


Figure 10: (i) Optical micrograph of HeLa cells ; (ii) fluorescence image after exposure to the medium/ether vehicle alone and (iii) after exposure to vehicle + SiNCs.

Figure 11 is an additional set of controls in which the fluorescence images are overlaid on the optical images. The false colour (orange-red) is chosen to mimic approximately the actual colour of the SiNC emission.

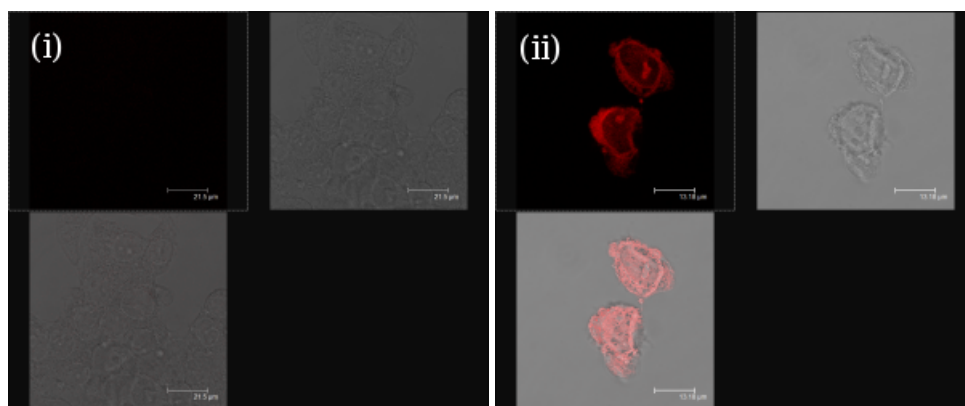


Figure 11: (i) Control, HeLa cells and (ii) with SiNCs. The optical and fluorescence images are overlaid in the bottom left hand corner of each part.

Finally, figure 12 shows a PL spectrum (excitation wavelength = 488 nm, Ar+ laser / Witec CRM200 confocal Raman microscope, Witec GmbH, Ulm, Germany). Although there is some batch-batch variation in peak wavelength of our SiNCs, we find that the emission spectrum from the SiNCs within the cells is substantially the same as from SiNCs in aqueous solution.

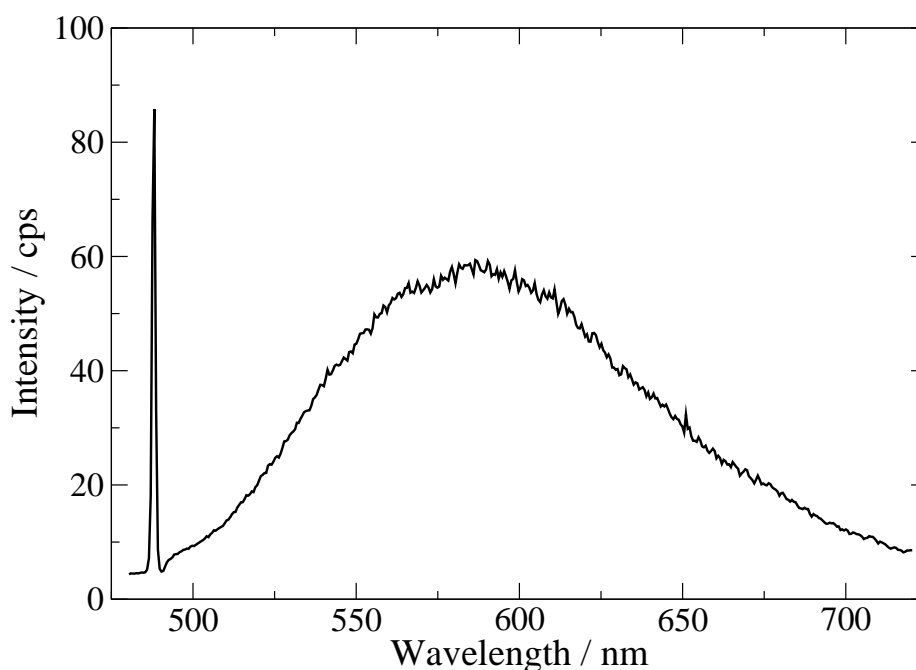


Figure 12: Photoluminescence spectrum with  $\lambda = 488$  nm excitation in a HeLa cell incubated with SiNCs for 4h.

## References

- [1] Y. Chao, L. Šiller, S. Krishnamurthy, P. R. Coxon, U. Bangert, M. Gass, L. Kjeldgaard, S. N. Patole, L. H. Lie, N. O'Farrell, T. A. Alsop, A. Houlton and B. R. Horrocks, *Nature Nanotech.* 2007, **2**, 486.
- [2] Y. Chao, S. Krishnamurthy, M. Montalti, L. H. Lie, A. Houlton, B. R. Horrocks, L. Kjeldgaard, V. R. Dhanak, M. R. C. Hunt and L. Šiller, *J. Appl. Phys.* 2005, **98**, 044316.
- [3] L. Šiller, N. Peltekis, S. Krishnamurthy, Y. Chao, S. J. Bull and M. R. C. Hunt, *Appl. Phys. Lett.* 2005, **86**, 221912.
- [4] L. C. P. M. de Smet, H. Zuilhof, E. J. R. Sudholter, L. H. Lie, A. Houlton and B. R. Horrocks, *J. Phys. Chem. B* 2005, **109**, 12020.
- [5] J. E. Bateman, R. D. Eagling, B. R. Horrocks and A. Houlton, *J. Phys. Chem. B* 2000, **104**, 5557.
- [6] M. E. Kompan, I. I. Novak, and V. B. Kulik, *J. Exp. Theor. Phys.* 2002, **94**, 739.
- [7] P. Mishra and K. P. Jain, *Mater. Sci. Eng. B* 2002, **95**, 202.
- [8] B. K. Patel, R. Mythili, R. Vijayalaxmi, R. K. Soni, S. N. Behera, and S. N. Sahu, *Physica B* 2002, **322**, 146.
- [9] X. G. Li, Y. Q. He and M. T. Swihart, *Langmuir* 2004, **20**, 4720.